Published in final edited form as:
Nat Protoc. 2013 December ; 8(12): . doi:10.1038/nprot.2013.140.

Synthesis of a probe for monitoring HSV1-*tk* reporter gene expression using chemical exchange saturation transfer MRI

Amnon Bar-Shir[1,2], **Guanshu Liu**[1,3], **Marc M Greenberg**[4], **Jeff W M Bulte**[1,2,3,5,6,7], and **Assaf A Gilad**[1,2,3]

[1]Division of Magnetic Resonance Research, Russell H. Morgan Department of Radiology and Radiological Science, the Johns Hopkins University School of Medicine, Baltimore, Maryland, USA

[2]Cellular Imaging Section and Vascular Biology Program, Institute for Cell Engineering, the Johns Hopkins University School of Medicine, Baltimore, Maryland, USA

[3]F.M. Kirby Research Center for Functional Brain Imaging, Kennedy Krieger Institute, Baltimore, Maryland, USA

[4]Department of Chemistry, the Johns Hopkins University, Baltimore, Maryland, USA

[5]Department of Biomedical Engineering, the Johns Hopkins University, Baltimore, Maryland, USA

[6]Department of Chemical and Biomolecular Engineering, the Johns Hopkins University, Baltimore, Maryland, USA

[7]Department of Oncology, the Johns Hopkins University School of Medicine, Baltimore, Maryland, USA

Abstract

In experiments involving transgenic animals or animals treated with transgenic cells, it is important to have a method to monitor the expression of the relevant genes longitudinally and noninvasively. An MRI-based reporter gene enables monitoring of gene expression in the deep tissues of living subjects. This information can be co-registered with detailed high-resolution anatomical and functional information. We describe here the synthesis of the reporter probe, 5-methyl-5,6-dihydrothymidine (5-MDHT), which can be used for imaging of the herpes simplex virus type 1 thymidine kinase (HSV1-*tk*) reporter gene expression in rodents by MRI. The protocol also includes data acquisition and data processing routines customized for chemical exchange saturation transfer (CEST) contrast mechanisms. The dihydropyrimidine 5-MDHT is synthesized through a catalytic hydrogenation of the 5,6-double bond of thymidine to yield 5,6-dihydrothymidine, which is methylated on the C-5 position of the resulting saturated pyrimidine ring. The synthesis of 5-MDHT can be completed within 5 d, and the compound is stable for more than 1 year.

Correspondence should be addressed to: A.A.G. (assaf.gilad@jhu.edu).

AUTHOR CONTRIBUTIONS A.B.-S., J.W.M.B. and A.A.G. were responsible for the study concept, design of experiments, data analysis and results interpretation. A.B.-S. and M.M.G. performed the chemical synthesis of the CEST probe. A.B.-S. and A.A.G. performed cloning, cell transfection, cell transplantation, *in vivo* MRI experiments and immunofluorescence. A.B.-S., G.L. and A.A.G. processed the CEST MRI data. A.B.-S., J.W.M.B. and A.A.G. wrote the protocol.

COMPETING FINANCIAL INTERESTS The authors declare no competing financial interests.

INTRODUCTION

Image-guided therapy has great potential for improving the treatment of various diseases, both in terms of drug development and drug delivery[1]. The ability to visualize therapeutic genes can revolutionize not only treatment management but also our understanding of complex biological processes. Hence, this technology has been evaluated for several decades in animal models and, recently, also in the clinic.

Certain genes can convert an inactive pro-drug to an active form only in transduced cells. These genes include the members of the deoxynucleoside kinase family, which can convert pro-drugs, such as ganciclovir and acyclovir, into active drugs[2]. Pioneering work by Tjuvajev *et al.*[3,4] and Gambhir *et al.*[5,6] transformed these therapeutic genes into diagnostic genes by designing probes for nuclear imaging of the enzyme herpes simplex virus type 1 thymidine kinase (HSV1-*tk*), thus making it a theranostic gene. HSV1-*tk* has been evaluated in the clinic both for imaging purposes[7,8] and as a therapeutic gene[9,10]. Years of practice have perfected the synthesis of the imaging probes and a large variety of applications into established protocols[11–16].

The radioactive-based tracers designed for imaging HSV1-*tk* enzyme expression with positron emission tomography (PET) and single-photon emission computed tomography (SPECT) are extremely sensitive and well established[17–20]. Indeed, PET and SPECT imaging modalities are much more sensitive than MRI. Nevertheless, the long shelf-life of an MRI probe, combined with the high spatial resolution that MRI can provide, could be used to gather additional morphological and functional information.

Recent advances in the field of molecular and cellular MRI have led to the development of new strategies in the design and synthesis of responsive MRI contrast agents[21–24] and reporter genes[25–27]. MRI-based reporter genes are unique among other genetically encoded reporters, owing to their ability to provide information about gene expression that can be co-registered with high-resolution (spatial resolution of 50–100 μm for *in vivo* rodent imaging) anatomical and functional information. Moreover, these genes enable the longitudinal study of the same subject with unlimited tissue penetration, and they have the potential for clinical translation. The CEST method is a novel approach for generating MRI contrast, in which the dynamic exchange process between an exchangeable proton and the surrounding water protons is used to amplify the desired contrast[28–30]. CEST MRI is being used for a wide range of applications, and it is particularly suitable for imaging enzyme activity[31–33], as well as gene expression[27,34,35].

Here we focus on the enzyme HSV1-TK (that is encoded by the HSV1-*tk* gene), which phosphorylates a wide range of nucleosides and their synthetic analogs. Before phosphorylation, these analogs facilitate transport mechanisms to cross the cell membrane. Once it has been phosphorylated by the HSV1-*tk*, the transported nucleoside becomes negatively charged and accumulates inside the cell[14]. The accumulation of high levels of the nucleosides in cells expressing HSV1-*tk*, and not in the surrounding tissue, makes the HSV1-*tk* a successful reporter gene for PET and SPECT applications[12–20,36], using a range of radiolabeled nucleotide analogs. In contrast, mammalian thymidine kinases do not phosphorylate these nucleoside analogs, making these substrates unique reporter probes for imaging HSV1-*tk* expression.

Here we describe in detail the synthesis of the CEST-MR imaging probe 5-MDHT (Fig. 1), the steps needed for expressing HSV1-*tk* in cells, methods for image acquisition and CEST data analysis.

The CEST-MRI reporter probe 5-MDHT is synthesized in four steps (Fig. 1). 5,6-Dihydrothymidine (compound **1**, Fig. 1) is obtained via catalytic hydrogenation of thymidine without further purification. Purification is carried out after the next step in which the hydroxyls (OH) of the 2′-deoxyribose moiety of the saturated thymidine are protected by silyl-based protecting groups (compound **2**, Fig. 1). This is followed by methylation of the C-5 position of the dihydropyrimidine ring (compound **3**, Fig. 1). Finally, the protecting groups are removed by reaction with fluoride ion, and the resulting 5-MDHT is purified using silica gel chromatography. For imaging rodents, tens of milligrams of the imaging probe will be sufficient for completing the study, which are quantities that can be reliably obtained with the synthetic steps described in this protocol. Note that for imaging HSV1-*tk* gene expression in larger subjects, larger quantities of 5-MDHT will be required. For such quantities, one should consider extra caution for the hydrogenation step, in which larger flasks will contain higher volumes of pressured H_2 gas. One should also exercise caution when carrying out the alkylation step, which uses pyrophoric alkyl lithium reagents.

Although the current protocol describes the synthesis of a dihydropyrimidine variant (5-MDHT) as an imaging probe for monitoring gene expression, diyhydrothymidine derivatives may be considered as CEST-MRI contrast agents for other molecular and cellular imaging applications[35]. Dihydropyrimidine derivatives may also be of interest for other scientific fields, as they have an important role in nucleic acid metabolism, DNA and RNA damage processes, as well as in the biosynthesis of t-RNA[37,38].

Although the current protocol describes the use of an MRI reporter probe for imaging the HSV1-*tk* reporter gene expression in a brain tumor model (9L rat glioma; Box 1) transplanted into a mouse brain, a variety of tumor cell lines and a diverse range of cell transplantation sites can be used with these same protocol steps. This protocol describes the basic CEST-MRI data acquisition and the CEST data processing steps (as schematically shown in Figure 2, with commonly used CEST definitions in Box 2) that are widely used in preclinical and clinical studies, but it also elaborates further on modifications and improvements from previously published imaging protocols[34].

Box 1

Cell and animal preparations

In this protocol, we describe how to use the MRI reporter probe to image HSV1-*tk* reporter gene expression in a brain tumor model (9L rat glioma) transplanted into a mouse brain. In this box we describe how the cells for this model are prepared and how they are injected into the mouse brain. A similar procedure could be used for different tumor models.

Transgenic cell preparation

For our work, we transfect and select a single HSV1-*tk*–expressing clone, as previously described in detail[34]. Transfect the 9L rat glioma cells with pcDNA3.1-HSV1-*tk* plasmid and with Lipofectamine 2000 as the transfection reagent. Select a single expressing clone using 0.5 mg ml^{-1} G418 antibiotics.

By using this approach, the preparation of a stable cell line starting from a single expressing clone, using 0.5 mg ml^{-1} G418 antibiotics, takes 2–4 weeks. Generation of a stable cell line from a pool of clones takes 1–2 weeks.

This protocol can be applied to a larger array of tumor cell lines and by using other transduction methods (i.e., different expressing vectors, lentiviruses, adenoviruses, etc.), as previously suggested[8,12,14–16].

Transgenic cell transplantation

For the brain tumor model that we use in our laboratory, stabilize the head of an adult NOD-SCID male mouse in a stereotaxic frame by using ear bars, and inoculate 2×10^5 HSV1-*tk*-expressing 9L cells ($9L^{HSV1\text{-}tk}$) and wild-type 9L cells ($9L^{wt}$) in 2 μl of saline bilaterally into the mouse striatum (coordinates: 0.0 mm posterior to bregma, 2.0 mm lateral to the midline, 3.0 mm ventral to the surface of the skull) to generate intracranial 9L tumors in both hemispheres.

This process takes 1 h per animal.

This protocol could be applied to cells that are xenografted into many different locations in the rodent body; however, the number of cells, the injected volume and time of tumor growth should be adjusted for each cell line and location used.

Box 2

Common definitions and parameters used in CEST-MRI

- S^0, MRI signal in the absence of a saturation pulse.
- $\Delta\omega$, chemical shift offset with respect to that of water protons ($\Delta\omega_{water} = 0$ p.p.m.).
- S, MRI signal in the presence of a saturation pulse applied at a particular offset ($\Delta\omega$ i.e., $S^{\Delta\omega}$).
- Z-spectrum, plot of the normalized water signal (S/S^0) as a function of saturation frequency $\Delta\omega$.
- MTR_{asym}, magnetization transfer ratio asymmetry, defined as $100 \times (S^{-\Delta\omega} - S^{\Delta\omega})/S^0$. It is the most common parameter used in CEST-MRI owing to its ability to remove the effect of direct water saturation, which is symmetric around the water resonance frequency (0.0 p.p.m.), thus improving CEST quantification.
- B_0, magnetic field strength of the MRI scanner used for the study.
- B_1, field strength of the applied radiofrequency saturation pulse (in Hz or μT units).
- t_{sat}, length (time) of the applied radiofrequency saturation pulse (in milliseconds).

The described MRI-based reporter system has several advantages, primarily the use of the new imaging probe, 5-MDHT, which has a long shelf life and is stable for a long time period in solution or powder form. This property makes it attractive for longitudinal studies, as well as for nanocarrier loading or sustained drug release systems that require multiple steps and which cannot be accomplished with a radioactive probe. Although the CEST MRI–based methodology has these advantages[35] with respect to imaging the HSV1-*tk* transgene, it is important to mention that CEST-MRI cannot achieve the high sensitivity of nuclear imaging–based strategies for monitoring gene expression. An interesting solution to this problem is to monitor HSV1-*tk* expression with MRI in combination with PET, which is particularly attractive given the recent availability of combined MR/PET scanners[39]. This innovative approach will provide the high sensitivity of PET for imaging HSV1-*tk*, combined with the repetitive acquisition of high-resolution HSV1-*tk* MR images, which can be overlaid on high-resolution anatomical MR images.

Experimental design

CEST MRI—Owing to the fact that CEST MRI contrast depends on the applied experimental parameters (especially on saturation pulse, B_1, power and length, see Box 2), it may be beneficial to consider optimizing the CEST parameters if other experimental models (different animal models, tumor cell lines, tumor injection sites and so on) are being used. In addition, it is important to note that the CEST contrast is also dependent on the magnetic field strength, B_0 (the use of an 11.7 T MRI scanner is described in the current protocol), and experimental parameters may need to be optimized for MRI scanners operating at a different magnetic field strength.

Animal models—It is highly recommended that control cells (either non-expressing HSV1-*tk* cells or cells that are expressing different control genes) be transplanted into the same animal (contralaterally to the HSV1-*tk*-expressing cells) and used as internal negative controls. This may help distinguish nonspecific CEST contrast. Alternatively, CEST contrast from the tumor region of interest (ROI) may be normalized to a well-defined ROI on nontumoral normal tissue, thus allowing the use of two different animal groups (expressing versus non-expressing HSV1-*tk*). By using the described protocol, one should have six subjects in each group to obtain statistically meaningful results; however, if a different experimental model is being used (different cell line, transgene transfection method, injection tumor site, etc.), a different experimental group size may be needed.

MATERIALS

REAGENTS

! CAUTION All reagent preparations and chemical reactions should be carried out with caution in a fume hood. Most of the reagents in this protocol are toxic or harmful and require the use of protective eyewear, gloves and a lab coat. In some steps, a face mask will be needed for protection.

- Hydrogen (H_2) cylinder **! CAUTION** Hydrogen is a flammable gas and is explosive. Avoid flames or other sources of heat around the reaction mixture. Perform all experiments in a fume hood and always wear eye protection.
- Argon (Ar) or nitrogen (N_2) cylinder
- Thymidine (Sigma-Aldrich, cat. no. T1895)
- Thin-layer chromatography (TLC) silica gel 60 F_{254} (Merck Millipore, cat. no. 1055540001)
- Magnesium sulfate ($MgSO_4$; Sigma-Aldrich, cat. no. M7506)
- Sodium bicarbonate ($NaHCO_3$; Sigma-Aldrich, cat. no. S6014)
- Sodium chloride (NaCl; Sigma-Aldrich, cat. no. S7653)
- Celite (Merck Millipore, cat. no. 102693) **! CAUTION** Celite is a carcinogen and an irritant. Wear a face mask when handling Celite and avoid dust formation.
- Silica gel 60 (Merck Millipore, cat. no. 109385)
- 5% Rh on alumina, 5 wt% loading, matrix alumina support; (Sigma-Aldrich, cat. no. 212857) **! CAUTION** This is a flammable solid.
- Imidazole (Sigma-Aldrich, cat. no. I3386) **! CAUTION** Imidazole is an irritant.
- *tert*-Butyldimethylsilyl chloride (TBDMSCl; Sigma-Aldrich, cat. no. 190500) **! CAUTION** This is a flammable solid and is corrosive.

- Ammonium chloride (NH_4Cl; Sigma-Aldrich, cat. no. 254134) **! CAUTION** Ammonium chloride is an irritant and is toxic.
- Iodomethane (CH_3I; Sigma-Aldrich, cat. no. I8507) **! CAUTION** Iodomethane is toxic, corrosive, a carcinogen and an irritant.
- *sec*-Butyllithium, 1.4 M in cyclohexane (Sigma-Aldrich, cat. no. 195596) **! CAUTION** *sec*-Butyllithium is a flammable liquid; it is pyrophoric and corrosive.
- Triethylamine trihydrofluoride (Sigma-Aldrich, cat. no. 344648) **! CAUTION** This reagent is toxic and corrosive.
- Anisaldehyde solution (Sigma-Aldrich, cat. no. SRA1-1KT) **! CAUTION** Anisaldehyde solution is a flammable liquid; it is toxic and corrosive. **! CAUTION** Avoid direct skin contact of organic solvents or acids and always wear gloves. As organic solvents are very flammable, perform heating procedures in dedicated flasks. ▲ **CRITICAL** All organic solvents and acids should be stored in dedicated chemical cabinets or in a fume hood.
- Ethyl ether (PHARMCO-AAPER, cat. no. zc3730000C) **! CAUTION** Ethyl ether is an irritant and is toxic.
- Methanol (PHARMCO-AAPER, cat. no. 339000) **! CAUTION** Methanol is a flammable liquid; it is an irritant and is toxic.
- Ethyl acetate (EtOAc; PHARMCO-AAPER, cat. no. 330000000) **! CAUTION** Ethyl acetate is a flammable liquid.
- Hexanes (PHARMCO-AAPER, cat. no. 359000) **! CAUTION** This reagent is flammable and an irritant.
- Dichloromethane (PHARMCO-AAPER, cat. no. 313000) **! CAUTION** Dichloromethane is a carcinogen and an irritant.
- Pyridine (Sigma-Aldrich, cat. no. 270970) **! CAUTION** Pyridine is a flammable liquid and a carcinogen.
- Acetone (PHARMCO-AAPER, cat. no. 329000000) **! CAUTION** Acetone is a flammable liquid and an irritant.
- Tetrahydrofuran (THF; PHARMCO-AAPER, cat. no. zh346000ANH) **! CAUTION** THF is a flammable liquid, a carcinogen and an irritant.
- Ethanol (Sigma-Aldrich, cat. no. 459844) **! CAUTION** Ethanol is a flammable liquid and an irritant.
- 2-Mercaptoethanol (Sigma-Aldrich, cat. no. M3148) **! CAUTION** 2-Mercaptoethanol is toxic, corrosive, a mutagen and a skin sensitizer.
- Acetic acid (Sigma-Aldrich, cat. no. 320099) **! CAUTION** Acetic acid is a combustible liquid and is corrosive.
- Sulfuric acid (H_2SO_4; Sigma-Aldrich, cat. no. 339741) **! CAUTION** Sulfuric acid is corrosive.
- Dry ice
- pcDNA3.1-HSV1-*tk*-V5 (custom-made)
- pLenti-CMV-HSV1-*tk*-V5 (custom-made)
- 9L rat glioma cell line

- RPMI 1640 medium (Life Technologies, cat. no. 11875-093)
- FBS (Fisher Scientific, cat. no. MT35015CV)
- L-Glutamine, 200 mM solution (Life Technologies, cat. no. 25030-164)
- Sodium pyruvate, 100 mM solution (Life Technologies, cat. no. 11360-070)
- Amphotericin B solution (Sigma-Aldrich, cat. no. A2942-100ML)
- Gentamycin, 50 mg ml^{-1} (Quality Biological, cat. no. 120-098-661)
- PBS, 10 mM, pH 7.4 (Life Technologies, cat. no. 20012-027)
- Saline solution, 0.9% (wt/vol) (Quality Biological, cat. no. 114-055-101)
- Isoflurane (Butler Schein, cat. no. 128183)
- Paraformaldehyde (PFA; Sigma-Aldrich, cat. no. 158127) **! CAUTION** PFA is a flammable solid; it is toxic, a skin sensitizer, an irritant and a carcinogen. Handle PFA in a fume hood with protective eyewear, facemask, gloves and a lab coat.
- 4′,6-diamidino-2-phenylindole (DAPI; Life Technologies, cat. no. D1306)
- Antibody diluent solution (Life Technologies, cat. no. 00-3118)
- V5 Mouse monoclonal antibody (Life Technologies, cat. no. R960-25)
- Alexa Fluor 594 goat anti-mouse IgG (H+L) (Life Technologies, cat. no. A-11005)
- Mounting medium, Fluoro-Gel (Electron Microscopy Sciences, cat. no. 17985-10)
- Mice (immune-deficient, 6–8-week-old male mice from in-house strains or from an appropriate provider) **! CAUTION** All involved personnel should be trained in animal handling. The animal protocol must be reviewed and approved by the institutional animal care and use committee before the experiment, and all animal experiments should be performed in accordance with the relevant guidelines and regulations of the approved protocol.
- BSA

EQUIPMENT

- Thick-walled hydrogen flasks
- H_2 pressure gauge
- Rotary evaporator
- Sintered glass
- Filter paper
- UV lamp (254 nm) for thin-layer chromatography
- Schlenk line
- Round-bottom flasks (50 ml and above)
- Separating funnels (250 ml and above)
- Glass columns
- Magnetic stir bars (adjusted in size to round-bottom flask)
- Collecting tubes, 15 ml

- Collecting tube rack
- Syringes, 1 ml
- Stereotaxic injection apparatus
- Hamilton syringes (10 μl–5 ml)
- Cell culture flasks (T25–T175)
- Isoflurane vaporizer
- MR scanner (i.e., Bruker 11.7T horizontal bore)
- MATLAB software (MathWorks)
- Cryostat
- Microscope slides (Fisher Scientific, cat. no. 12-550-19)
- Microscope coverslip (Fisher Scientific, cat. no. 12-545-M)
- Fluorescent microscope

REAGENT SETUP

$NaHCO_3$ saturated solution—Dissolve 90 g of $NaHCO_3$ in 1 liter of water. Store the solution at room temperature (22–25 °C) in a closed bottle for 1 year.

NH_4Cl saturated solution—Dissolve 55 g of NH_4Cl in 1 liter of water. Store the solution at room temperature in a closed bottle for 1 year.

***p*-Anisaldehyde solution—**To 135 ml of ethanol, 5 ml of concentrated H_2SO_4 and 1.5 ml of acetic acid, add 3.7 ml of *p*-anisaldehyde (PAA) solution. ▲ **CRITICAL** The solution should be stored at 20–25 °C in a 100-ml wide-mouth jar wrapped with aluminum foil to ensure a long shelf life.

PFA solution, 4% (wt/vol) in PBS—Dissolve 40 g of PFA in 1 liter of PBS. Adjust the pH of the resulting solution to 7.4. ▲ **CRITICAL** 4% (wt/vol) PFA should be freshly prepared before use. However, if storage is required, 50-ml aliquots may be stored at −20 °C for several weeks. ▲ **CRITICAL** Perform all experiments that relate to cell preparation using sterile techniques.

9L cell medium—9L cell medium contains 500 ml of 1640 RPMI, 5 ml of L-glutamine solution, 5 ml of sodium pyruvate solution, 0.6 ml of gentamycin, 5 ml of amphotericin B solution and 1.7 μl of 2-mercaptoethanol. Store it at 4 °C for up to 3 months.

DAPI solution—Prepare a stock solution of 5 mg DAPI in 1 ml of dH_2O. Dilute 5 μl of DAPI stock solution in 10 ml of dH_2O to prepare a DAPI working solution. ▲ **CRITICAL** DAPI working solution should be stored at 4 °C in a 50-ml tube wrapped with aluminum foil to prevent light.

EQUIPMENT SETUP

MR scanner—The MR scanner should be set up according to the manufacturer's instructions. A horizontal-bore, 7-, 9.4- or 11.7-Tesla MRI system is preferred for better animal access; however, a vertical MRI scanner can be used as well. The MR spectrometer should be equipped with an animal holder specifically designed for mouse brain imaging. Note that a volume radiofrequency (RF) coil is preferable for CEST-MRI experiments in

order to achieve a homogenous B_1. Mice are initially placed in an induction chamber containing 4% (wt/vol) isoflurane. They are then positioned in the scanner, and kept anesthetized with an isoflurane vaporizer (~1–2% (wt/vol) isoflurane with air or oxygen) attached to a nose cone. ▲ **CRITICAL** An MRI-compatible respiration rate monitoring system should be used to ensure that the mouse's respiration rate is maintained at 30–60 breaths per min by adjusting the dose of anesthesia using the vaporizer.

PROCEDURE

Production of 5-MDHT, part 1: synthesis of 5,6-dihydrothymidine (1) ● TIMING 2 h

1| Weigh thymidine (517 mg, 2.06 mmoles) into a thick-walled flask containing a magnetic stirring bar, and dissolve it in a 32-ml solution of water and methanol (1:1 by volume).

? TROUBLESHOOTING

2| Add 75 mg of catalyst, 5% Rh on alumina (5 wt% loading, matrix alumina support), to the reaction mixture and stir it vigorously to generate a homogenous suspension.

3| Equip the reaction flask with an appropriate pressure gauge for controlling pressure and fill it with 50 p.s.i. of H_2. **! CAUTION** Prevent flames around the reaction mixture. H_2 gas is explosive. Perform all experiments in a fume hood and wear eye protection.

4| Evacuate the H_2 gas and repeat filling and evacuating H_2 three times to flush traces of oxygen.

5| Fill the reaction flask with 50 p.s.i. of H_2 and stir the reaction mixture for 2 h at room temperature.

6| Cautiously evacuate the H_2 gas, remove the pressure gauge and withdraw 50 μl of the reaction mixture for monitoring the reaction for completion. Place a drop from the reaction mixture on a silica gel–coated TLC plate, dry it and confirm the disappearance of the thymidine spot under UV light, indicating reaction completion. Use a solution of thymidine (20 mg in 3 ml methanol) as positive control. Note that a loss of UV activity is obtained when thymidine is converted to 5,6-dihydrothymidine. There is no need to run the TLC plate in a developing chamber.

7| If required (uncompleted reaction as determined by TLC, Step 6), equip the reaction flask with the pressure gauge (Step 3) and refill it with 50 p.s.i. of H_2. Repeat Steps 4–6 until the reaction is complete.

8| Add Celite to a sintered glass filter (an ~2-cm-thick layer) and wash it three times with 30 ml of methanol each time. Increase the rate of methanol passage through the Celite by either forcing the solvent through, using air, or filtering under a vacuum, using an aspirator.

9| Pour the reaction mixture (Steps 5 and 6, after the reaction is complete) onto the Celite-containing filter (Step 8), and wash it three times with 30 ml of methanol to recover the product and separate it from the catalyst.

10| Transfer the filtrate to a round-bottom flask and remove the solvent using a rotary evaporator. Heat the evaporating solution in a water bath (50 °C) to allow complete removal of the water from the reaction mixture.

? TROUBLESHOOTING

11| Proceed to the next step (Step 12) using the crude product without further purification.

■ **PAUSE POINT** Flush the round-bottom flask containing the crude product (Step 10) with argon (or nitrogen) gas, seal it with Parafilm and store it at 4 °C for future experiments.

Production of 5-MDHT, part 2: azeotropic drying of 5,6-dihydrothymidine (1) ● TIMING 3–5 h

12| Weigh 0.5 g (2.05 mmoles, 1 equivalent) of 5,6-dihydrothymidine (**1**) into a 50-ml round-bottom flask equipped with a magnetic stirring bar.

13| Add 4 ml of dry pyridine and equip the flask with a vacuum/inert gas adaptor and place the flask in a water bath at room temperature.

14| Connect the flask to a Schlenk line, stir the reaction mixture to dissolve 5,6-dihydrothymidine (**1**) and purge it with argon (or nitrogen) gas.

15| Open the system to high vacuum until all the solvent is removed (~3–5 h).

16| Vent the flask to argon (or nitrogen) gas.

! CAUTION Place the vacuum system in a fume hood and wear safety glasses for protection when you are working with a high-vacuum system.

Production of 5-MDHT, part 3: synthesis of 3′,5′-*O*-bis(*tert*-butyldimethylsilyloxy)5,6-dihydrothymidine (2) ● TIMING variable; purification takes 2–3 h

17| Add 10 ml of dry pyridine to 0.5 g (2.05 mmoles, 1 equivalent) of azeotropically dried 5,6-dihydrothymidine (**1**, Steps 11–15).

? TROUBLESHOOTING

18| Quickly add 0.73 g (10.7 mmoles, 5.2 equivalents) of imidazole and 0.77 g (5.1 mmoles, 2.5 equivalents) of TBDMSCl to the stirred solution in Step 17.

19| Flush the reaction mixture with argon (or nitrogen) gas and stir the reaction mixture under an argon (or nitrogen) gas atmosphere.

20| Monitor the reaction progress by TLC after a ‘mini work-up’ step, as follows: transfer 50 μl of the reaction mixture, via a dry syringe, to a 1.5-ml plastic tube and add 0.5 ml of saturated $NaHCO_3$ solution and 0.5 ml of ethyl acetate. Mix the contents well to extract, let the tube sit for phase separation, and then spot, on a TLC plate, one drop from the top organic layer. Develop the plate in a developing jar with a mixture of EtOAc/hexanes (4:1 volume ratio). Monitor the reaction progress by staining the TLC plate with PAA solution after heating the plate. The R_f values are 0.75 for the product and 0.25 for the mono-TBDMS compound.

21| After verification of reaction completion using TLC (Step 20), add 20 ml of saturated $NaHCO_3$ solution and 20 ml of water to terminate the reaction. Pour the resulting mixture into a 150-ml separating funnel.

22| Extract three times with 20 ml of diethyl ether and combine the organic phase layers (top layer).

23| Wash the combined organic phase with 50 ml of brine, dry the organic phase using $MgSO_4$, filter it through a filter paper and remove the solvent using a rotary evaporator. No heating of the evaporating solution is required.

24| Load the crude product onto a silica gel column (1:50 weight ratio of crude: silica gel) and separate the main product from the reagents and by-product(s) by using a mixture of EtOAc/hexanes (4:1 volume ratio) as the eluent.

25| Collect fractions (~10 ml) until the compound is completely eluted (determine by TLC, see Step 20), combine the fractions containing the product and evaporate the solvent by using a rotary evaporator. To validate the synthesis of pure 3′,5′-*O*-bis(*tert*-butyldimethylsilyloxy)-5,6-dihydrothymidine (**2**), dry the product under high vacuum, perform ^{1}H-NMR and compare the spectrum with previously published ^{1}H-NMR data[40,41].

? TROUBLESHOOTING

■ **PAUSE POINT** Flush the product with argon (or nitrogen) gas, seal it with Parafilm and store it at 4 °C for future experiments.

Production of 5-MDHT, part 4: synthesis of 3′,5′-*O*-bis(*tert*-butyldimethylsilyloxy)-5-methyl-5,6-dihydrothymidine (3) ● TIMING 6–7 h

26| Distill 1 ml of iodomethane (CH_3I), boiling point 41–43 °C, under an argon (or nitrogen) gas atmosphere. Collect the dry distilled iodomethane and seal it with Parafilm for use in the next step.

? TROUBLESHOOTING

27| Weigh 0.7 g (1.5 mmoles, 1 equivalent) of 3′,5′-*O*-bis(*tert*-butyldimethylsilyloxy)-5,6-dihydrothymidine (**2**) into a 50-ml round-bottom flask equipped with a magnetic stir bar, dissolve it in 2 ml of pyridine and azeotropically dry it as described in Steps 12–16.

28| After removing all pyridine, equip the reaction flask with a septum and add 15 ml of THF, dissolve compound **2** and cool the reaction flask to −78 °C by using dry ice/acetone.

29| Use a dry syringe to carefully add 2.7 ml of *sec*-butyllithium (*sec*-BuLi) solution (1.4 M in cyclohexane, 3.75 mmoles, 2.5 equivalents) over a 5-min period. Stir the flask for 1 h at −78 °C.

30| Add 0.14 ml of distilled iodomethane (Step 25, 2.25 mmoles, 1.5 equivalents) to the stirred reaction mixture (Step 29) and leave it at −78 °C for 1 additional hour.

31| Warm the reaction to room temperature and quench it with 200 ml of saturated NH_4Cl solution.

32| Extract the resulting mixture three times with 250 ml of EtOAc. Combine the organic phases and wash the mixture with 500 ml of brine, dry it over Na_2SO_4, filter it through a filter paper and remove the organic solvent with a rotary evaporator.

33| Dilute 10 μl of crude product (in 100 μl hexanes), spot the solution using a capillary tube on the TLC plate and run it in a developing chamber by using an EtOAc/hexanes mixture (1:4 volume ratio). Check the plate using PAA solution. The R_f values are 0.3 for the dimethyl product (**3**) and 0.2 for the unreacted compound **2**.

? TROUBLESHOOTING

34| Load the crude product onto a silica gel column (1:100 weight ratio of crude:silica gel) and separate the main product from reagents and by-products by a mixture of EtOAc/hexanes mixture (1:4 volume ratio) as the eluent.

? TROUBLESHOOTING

35| Collect fractions (~10 ml) until the compound is completely eluted (determine by using TLC, see Step 33), combine the fraction containing the product and evaporate the solvent by using a rotary evaporator (no heating of the evaporating solution is required). Dry the product under high vacuum, perform ^{1}H-NMR and compare the spectrum with previously published ^{1}H-NMR data[42] to validate pure 3′,5′-*O*-bis(*tert*-butyldimethylsilyloxy)-5-methyl-5,6-dihydrothymidine (**3**).

? TROUBLESHOOTING

■ **PAUSE POINT** Flush the product with argon (or nitrogen) gas, seal it with Parafilm and store it at 4 °C for future experiments.

Production of 5-MDHT, part 5: synthesis of 5-MDHT ● TIMING 4–5 h

36| In a 25-ml round-bottom flask equipped with a magnetic stir bar, dissolve 0.55 g (1.1 mmoles, 1 equivalent) in 10 ml of dry THF.

? TROUBLESHOOTING

37| Use a syringe to add 0.93 ml (5.5 mmoles, 5 equivalents) of triethylamine trihydrofluoride; stir the reaction mixture for 1 additional hour.

38| Monitor the reaction progress and completion by TLC, by using a dichloromethane/methanol mixture (92:8 volume ratio). Check the plate using PAA solution. The R_f value of the product is 0.25.

? TROUBLESHOOTING

39| After the reaction is complete, remove the solvent with a rotary evaporator (no heating of the evaporating solution is required), load the crude product onto a silica gel column (1:50 weight ratio of crude:silica gel) and separate the main product from reagents and by-products by using a dichloromethane/methanol mixture (92:8 volume ratio) as the eluent.

? TROUBLESHOOTING

40| Collect the fractions (~10 ml) until the compound is completely eluted (determine by using TLC; see Step 38), combine the fraction containing the product and evaporate the solvent with a rotary evaporator (no heating of the evaporating solution is required). Dry the product under high vacuum, perform ^{1}H-NMR and compare the spectrum with ^{1}H-NMR results (see ANTICIPATED RESULTS) to validate pure 5-MDHT.

? TROUBLESHOOTING

■ **PAUSE POINT** Flush the product with argon (or nitrogen) gas, seal it with Parafilm and store it at 4 °C for future experiments.

MRI data acquisition and processing, part 1: probe injection, animal localization and tumor identification ● TIMING 15–20 min per subject

41| Solubilize 5-MDHT in saline to a final concentration of 25 mg ml^{-1} and filter the solution through a 0.2-μm filter.

42| Weigh the mouse and inject 5-MDHT solution (Step 41) through the tail vein to a final amount of 150 mg kg^{-1} body weight. Place the mouse back into the cage for 2 h.

! CAUTION Do not exceed an injection volume of 0.2 ml per mouse in one bolus.

43| Two hours after probe injection, anesthetize the mouse with 2–3% (wt/vol) isoflurane air gas; restrain the mouse in a holder, centering at both the center of the RF coil and the center of the magnet. Keep the mouse anesthetized throughout the imaging procedure using 1.5% (wt/vol) isoflurane gas inhalation.

! CAUTION At least one of the physiological parameters, such as respiration or body temperature, must be closely monitored, and the percentage of isoflurane should be adjusted accordingly to maintain a proper state of anesthesia.

44| Determine the appropriate slice to image by using a localizer sequence, such as tripilot RARE, available for the Bruker MRI scanners.

45| Adjust the B_0 shimming to a satisfactory level by using either an automatic shimming protocol, such as FieldMAP (Bruker), or by performing manual shimming.

! CAUTION Do not forget to readjust the resonance frequency offset back to 0 after adjusting shimming.

? TROUBLESHOOTING

46| Acquire T_2-weighted anatomical images by using a multiple-slice fast-spin echo (SE) sequence (e.g., RARE for the Bruker MRI scanner), and identify subsequent regions of interest for single-slice CEST imaging. The following typical parameters can be used: acquisition bandwidth = 75 kHz; 15 slices; 0.7 mm slice thickness; echo time (TE) as short as possible (~ 4–5 ms); TR = 2,000 ms; RARE factor (echo number) = 16; field of view (FOV) = 20 mm × 20 mm; and matrix size = 128 × 64.

47| Localize a 1.0-mm slice in the ROI in which both tumors are observed on the MR image. Acquire high-resolution, T_2-weighted anatomical images with the following parameters: TR/TE = 5,000/4 ms; RARE factor of 16; FOV = 16 mm × 16 mm and matrix size = 256 × 128.

MRI data acquisition and processing, part 2: CEST data acquisition

48| MTR_{asym} values (Box 2) are the most common metrics for quantifying CEST-weighted images. If a relatively short experiment time is required (e.g., measuring fast dynamic changes), one can calculate the MTR_{asym} maps from CEST-weighted image sets (option A) at $\Delta\omega = 5.0$ p.p.m. ($S^{+5\ \text{p.p.m.}}$) and $\Delta\omega = -5.0$ p.p.m. ($S^{-5\ \text{p.p.m.}}$). For improved quality of the CEST data, the acquisition of CEST spectral images, i.e., Z-spectra (option B), is highly recommended.

(A) Acquisition of CEST-weighted image sets with interleaved saturation offsets ● TIMING 15–20 min

i. Use the same slice geometry used in Step 47 for CEST-weighted images. Modify a fast SE protocol (e.g., a RARE sequence on the Bruker scanner) by including a magnetization transfer module with the following parameters: a single base pair–shaped saturation pulse, B_1/t_{sat} = 213 Hz/4,000 ms.

ii. Acquire four sets of CEST-weighted images ($S^{+5\ p.p.m.}$; $S^{-5\ p.p.m.}$) with TR/TE = 6,000/35 ms and a matrix of 128 × 48. Each set contains two CEST-weighted images ($S^{+5\ p.p.m.}$ or $S^{-5\ p.p.m.}$).

(B) Acquisition of CEST spectral images (Z-spectra) ● TIMING ~50–60 min

i. Use the same slice geometry and the same CEST imaging protocol described in option A.

ii. Acquire CEST spectral images (Z-spectra) by sweeping the offsets of the saturation pulse in the modified CEST-weighted imaging protocol from −6.0 p.p.m. to +6.0 p.p.m. with respect to the water resonance (0 p.p.m.), in increments of 0.2 p.p.m. Acquire the images in an interleaved pattern, i.e., $S^{+6.0\ p.p.m.}$, $S^{-6.0\ p.p.m.}$, $S^{+5.8\ p.p.m.}$, $S^{-5.8\ p.p.m.}$… $S^{0.0\ p.p.m.}$, to minimize effects from B_0 drift that may occur during a long acquisition time.

iii. Acquire an S^0 image with the same protocol and parameters used for CEST-weighted images, except for setting the saturation field to $B_1 = 0$ (without saturation).

iv. Run a water saturation shift referencing (WASSR) imaging procedure for estimation and correction of B_0 inhomogeneities[43]. Use the same protocol and parameters as used for CEST spectral imaging acquisition (previous step), except for TR = 1,500 ms, B_1/t_{sat} = 21 Hz/500 ms, with a sweep range from −1.0 to +1.0 p.p.m. (0.1-p.p.m. steps).

? TROUBLESHOOTING

MRI data acquisition and processing—CEST data processing ● TIMING 15–30 min per subject

▲ **CRITICAL** A MATLAB-based CEST data processing toolbox for analyzing CEST data is available at the F.M. Kirby Research Center for Functional Brain Imaging website: http://godzilla.kennedykrieger.org/. Note that the CEST Data Processing procedure can be performed in any other image-processing software in addition to MATLAB.

49| The data-processing procedure should match the chosen data-acquisition procedure (Step 48A or 48B).

(A) Data processing of CEST images acquired using the $S^{+5\ p.p.m.}$; $S^{-5\ p.p.m.}$ pattern

i. Average CEST-weighted images acquired at $S^{+5\ p.p.m.}$, i.e., S^+.

ii. Average CEST-weighted images acquired at $S^{-5\ p.p.m.}$, i.e., S^-.

iii. Calculate the MTR_{asym} map defined by $MTR_{asym} = 100 \times (S^- - S^+)/S^-$.

iv. Calculate the CEST contrast change, ΔMTR_{asym}, in a ROI, defined as [MTR_{asym} (tumor)] − [MTR_{asym} (normal tissue)].

(B) Data processing of CEST spectral images (Z-spectra)

i. Estimate the B_0 inhomogeneities (δB_0 map) on a voxel-by-voxel basis by fitting WASSR spectral data (normalized without saturation, i.e., $S_{norm} = S/S^0$) at each $\Delta\omega$ to a Lorentzian shape by the formula: $S_{norm}=[A/(1+B/(\Delta\omega-\delta B_0)]+C$, where A, B and C are constants.

ii. By using the δB_0 produced above, correct the offsets of CEST spectral images on a voxel-by-voxel basis. This can be done by producing a new set of CEST-spectral images at the offsets of interest by using a spline interpolation algorithm, which is included in the MATLAB imaging processing toolbox.

iii. Analyze the CEST contrast at a particular offset ($\Delta\omega$) to obtain the MTR_{asym}, defined by $MTR_{asym} = 100 \times (S^{-\Delta\omega} - S^{\Delta\omega})/S^0$.

iv. Calculate the CEST contrast change, ΔMTR_{asym}, in any ROI, defined as [MTR_{asym} (tumor)] − [MTR_{asym} (normal tissue)].

50| Determine the threshold for separating the pixels with high CEST contrast from those with background CEST contrast with either a global contrast-to-noise-ratio filtering (i.e., $\mathrm{CNR} > 2\sqrt{2}$) or by manual adjustment based on the histogram plot of the produced MTR_{asym} map.

51| Overlay the thresholded (Step 50) MTR_{asym} map (or CEST map) onto the high-resolution T_2-weighted image obtained in Step 47 to determine the localization of the highest CEST contrast.

Histological validation of HSV1-TK expression ● TIMING 2 d

52| Perfuse the imaged mice transcardially with 10 mM PBS; follow this by 4% (wt/vol) PFA fixation. Remove the brain carefully and postfix it in 4% (wt/vol) PFA overnight.

53| Cryopreserve the brains by submerging them in 50 ml of a 30% (wt/vol) sucrose solution (in PBS) for 24–48 h, and then freeze the tissue on dry ice.

■ **PAUSE POINT** Frozen brains can be stored for 1 year at −80 °C.

54| Quickly transfer the frozen brain into a precooled cryostat chamber (−21 °C). Allow the tissue temperature to equilibrate and mount the tissue on a specimen holder.

55| Cut 30-μm-thick slices and mount the slices from the regions of interest (tumor) on microscope slides.

56| Block the slices on slides for 1 h at room temperature with PBS containing 5% (wt/vol) BSA; follow this by overnight incubation (4 °C) in anti-V5 antibody solution (1:500 dilution in an antibody diluent reagent solution).

57| Wash the slides three times for 5 min with PBS, and incubate them for 1 h with an appropriate secondary fluorescent antibody (for example, Alexa Fluor 594 goat anti-mouse IgG (H+L), 1:400 dilution, in a blocking solution). Wash the slides three times for 5 min with PBS and stain them for nuclei with 1 μg ml^{-1} DAPI solution for 10 min.

58| Wash the DAPI solution with PBS, apply mounting medium and cover the slides with a coverslip.

■ **PAUSE POINT** Slides may be stored for 2–3 months at 4 °C in the dark for further analysis.

59| Confirm the expression of the HSV1-*tk* fused to V5 by evaluating the immunofluorescence staining of the tumor of interest (Fig. 3).

? TROUBLESHOOTING

Troubleshooting advice can be found in Table 1.

● TIMING

Steps 1–11, production of 5-MDHT, part 1: synthesis of 5,6-dihydrothymidine (**1**): the reaction should be completed in 2 h, as determined by TLC

Steps 12–16, production of 5-MDHT, part 2: azeotropic drying of 5,6-dihydrothymidine (**1**): azeotropic drying should take 3–5 h (depending on the solvent volume and the vacuum pressure in the system)

Steps 17–25, production of 5-MDHT, part 3: synthesis of 3′,5′-*O*-bis(*tert*-butyldimethylsilyloxy)5,6-dihydrothymidine (**2**): reaction time may vary and should be monitored (by TLC, Step 20) starting at 2 h of reaction. The purification of the product with a silica gel column takes 2–3 h

Steps 26–35, production of 5-MDHT, part 4: synthesis of 3′,5′-*O*-bis(*tert*-butyldimethylsilyloxy)-5-methyl-5,6-dihydrothymidine (**3**): 6–7 h

Steps 36–40, production of 5-MDHT, part 5: synthesis of 5-MDHT: 4–5 h

Steps 41–47, MRI data acquisition and processing, part 1: animal localization and tumor identification: for animal localization, appropriate geometry determination, B_0 shimming and acquisition of T_2-weighted images (Steps 43–47), 15–20 min per subject

Step 48A, acquisition of CEST-weighted image sets with the saturation offsets interleaved at $\Delta\omega = 5.0$ p.p.m. ($S^{+5\ \text{p.p.m.}}$) and $\Delta\omega = 5.0$ p.p.m. ($S^{-5\ \text{p.p.m.}}$): CEST acquisition with four sets of $S^{+5\ \text{p.p.m.}}$, $S^{-5\ \text{p.p.m.}}$ takes 15–20 min

Step 48B, acquisition of CEST spectral images (Z-spectra): ~50–60 min

Steps 49–51, MRI data acquisition and processing—CEST data processing: 15–30 min per subject

Steps 52–59, histological validation of HSV1-TK expression: 2 d

ANTICIPATED RESULTS

Preparation of 5,6-dihydrothymidine (1)—The conversion of thymidine to compound **1** (Steps 1–10) should be completed within 2 h; however, the reaction mixture may be stirred overnight if desired, for up to 18 h (as determined by TLC, Step 6). In case of poor conversion, refer to TROUBLESHOOTING.

Preparation and purification of 3′,5′-*O*-bis(*tert*-butyldimethylsilyloxy)-5,6-dihydrothymidine (2)—The overall yield for compound **2** should be 75%. TLC: EtOAc/hexanes mixture (4:1 volume ratio), $R_f = 0.75$. In case of poor yield, refer to TROUBLESHOOTING. See previously published ^{1}H-NMR results[40,41] and compare them with your ^{1}H-NMR data.

Preparation and purification of 3′,5′-*O*-bis(*tert*-butyldimethylsilyloxy)-5-methyl-5,6-dihydrothymidine (3)—The overall yield for compound **3** should be 70%. TLC: EtOAc/hexanes mixture (1:4 volume ratio), $R_f = 0.3$. In case of poor yield, refer to TROUBLESHOOTING. See previously published ^{1}H-NMR results[42] and compare with your ^{1}H-NMR data.

Preparation and purification of 5-MDHT—The overall yield for 5-MDHT should be 70% after two silica gel columns. TLC: dichloromethane/methanol mixture (92:8 volume ratio), $R_f = 0.25$. ^{1}H NMR (500 MHz, D_2O) δ 6.26 (t, 1H, $J = 7.3$ Hz), 4.37 (m, 1H), 3.91 (m, 1H), 3.79 (dd, 1H, $J = 12.2$ Hz, $J = 4$ Hz), 3.76 (dd, 1H, $J = 12.2$ Hz, $J = 5.5$ Hz), 2.29 (m, 1H), 2.15 (m, 1H), 1.22 (s, 6H). In case of poor yield, refer to TROUBLESHOOTING.

CEST-MRI—CEST-MRI contrast difference between wild-type tumor and HSV1-*tk*–expressing tumors. A concentration of 0.5–1.0 mM of 5-MDHT should be accumulated to generate significant CEST contrast in HSV1-*tk*–expressing cells compared with controls at the frequency offset of the imino exchangeable proton of 5-MDHT (Fig. 4).

Acknowledgments

This study was supported by grant nos. U54CA151838 (US National Institutes of Health (NIH)), MSCRFF-0103-00 (Maryland Stem Cell Research Fund), NIH 2R01 NS045062 and GM-054996 (NIH). We thank M. McAllister for her assistance in editing the manuscript.

References

1. Yigit MV, Moore A, Medarova Z. Magnetic nanoparticles for cancer diagnosis and therapy. Pharmacol Res. 2012; 29:1180–1188.
2. Culver KW, et al. *In vivo* gene transfer with retroviral vector-producer cells for treatment of experimental brain tumors. Science. 1992; 256:1550–1552. [PubMed: 1317968]
3. Tjuvajev JG, et al. Imaging herpes virus thymidine kinase gene transfer and expression by positron emission tomography. Cancer Res. 1998; 58:4333–4341. [PubMed: 9766661]
4. Tjuvajev JG, et al. Noninvasive imaging of herpes virus thymidine kinase gene transfer and expression: a potential method for monitoring clinical gene therapy. Cancer Res. 1996; 56:4087–4095. [PubMed: 8797571]
5. Gambhir SS, et al. Imaging adenoviral-directed reporter gene expression in living animals with positron emission tomography. Proc Natl Acad Sci USA. 1999; 96:2333–2338. [PubMed: 10051642]
6. Gambhir SS, et al. A mutant herpes simplex virus type 1 thymidine kinase reporter gene shows improved sensitivity for imaging reporter gene expression with positron emission tomography. Proc Natl Acad Sci USA. 2000; 97:2785–2790. [PubMed: 10716999]
7. Jacobs A, et al. Positron-emission tomography of vector-mediated gene expression in gene therapy for gliomas. Lancet. 2001; 358:727–729. [PubMed: 11551583]
8. Yaghoubi SS, et al. Noninvasive detection of therapeutic cytolytic T cells with 18F-FHBG PET in a patient with glioma. Nat Rev Clin Oncol. 2009; 6:53–58.
9. Freytag SO, et al. Phase I study of replication-competent adenovirus-mediated double-suicide gene therapy for the treatment of locally recurrent prostate cancer. Cancer Res. 2002; 62:4968–4976. [PubMed: 12208748]
10. Freytag SO, et al. Five-year follow-up of trial of replication-competent adenovirus-mediated suicide gene therapy for treatment of prostate cancer. Mol Ther. 2007; 15:636–642. [PubMed: 17228316]
11. Miyagawa T, et al. Imaging of HSV-*tk* reporter gene expression: comparison between [18F]FEAU, [18F]FFEAU, and other imaging probes. J Nucl Med. 2008; 49:637–648. [PubMed: 18344433]
12. Sun N, Lee A, Wu JC. Long term non-invasive imaging of embryonic stem cells using reporter genes. Nat Protoc. 2009; 4:1192–1201. [PubMed: 19617890]
13. Yaghoubi SS, Berger F, Gambhir SS. Studying the biodistribution of positron emission tomography reporter probes in mice. Nat Protoc. 2007; 2:1752–1755. [PubMed: 17641641]
14. Yaghoubi SS, Gambhir SS. Measuring herpes simplex virus thymidine kinase reporter gene expression *in vitro*. Nat Protoc. 2006; 1:2137–2142. [PubMed: 17487205]
15. Soghomonyan S, et al. Molecular PET imaging of HSV1-*tk* reporter gene expression using [18F]FEAU. Nat Protoc. 2007; 2:416–423. [PubMed: 17406603]
16. Yaghoubi SS, Gambhir SS. PET imaging of herpes simplex virus type 1 thymidine kinase (*HSV1-tk*) or mutant *HSV1-sr39tk* reporter gene expression in mice and humans using [18F]FHBG. Nat Protoc. 2006; 1:3069–3075. [PubMed: 17406570]
17. Burton JB, et al. Adenovirus-mediated gene expression imaging to directly detect sentinel lymph node metastasis of prostate cancer. Nat Med. 2008; 14:882–888. [PubMed: 18622403]

18. Hung SC, et al. Mesenchymal stem cell targeting of microscopic tumors and tumor stroma development monitored by noninvasive *in vivo* positron emission tomography imaging. Clin Cancer Res. 2005; 11:7749–7756. [PubMed: 16278396]
19. Willmann JK, et al. Imaging gene expression in human mesenchymal stem cells: from small to large animals. Radiology. 2009; 252:117–127. [PubMed: 19366903]
20. Wu JC, Inubushi M, Sundaresan G, Schelbert HR, Gambhir SS. Positron emission tomography imaging of cardiac reporter gene expression in living rats. Circulation. 2002; 106:180–183. [PubMed: 12105155]
21. Lubag AJ, De Leon-Rodriguez LM, Burgess SC, Sherry AD. Noninvasive MRI of beta cell function using a Zn2+-responsive contrast agent. Proc Natl Acad Sci USA. 2011; 108:18400–18405. [PubMed: 22025712]
22. Loving GS, Mukherjee S, Caravan P. Redox-activated manganese-based MR contrast agent. J Am Chem Soc. 2013; 135:4620–4623. [PubMed: 23510406]
23. Osborne EA, Jarrett BR, Tu C, Louie AY. Modulation of T2 relaxation time by light-induced, reversible aggregation of magnetic nanoparticles. J Am Chem Soc. 2010; 132:5934–5935. [PubMed: 20373802]
24. Catanzaro V, et al. A R_{2p}/R_{1p} ratiometric procedure to assess matrix metalloproteinase-2 activity by magnetic resonance imaging. Angew Chem Int Ed Engl. 2013; 52:3926–3930. [PubMed: 23450786]
25. Cohen B, et al. MRI detection of transcriptional regulation of gene expression in transgenic mice. Nat Med. 2007; 13:498–503. [PubMed: 17351627]
26. Genove G, DeMarco U, Xu H, Goins WF, Ahrens ET. A new transgene reporter for *in vivo* magnetic resonance imaging. Nat Med. 2005; 11:450–454. [PubMed: 15778721]
27. Gilad AA, et al. Artificial reporter gene providing MRI contrast based on proton exchange. Nat Biotech. 2007; 25:217–219.
28. Ward KM, Aletras AH, Balaban RS. A new class of contrast agents for MRI based on proton chemical exchange dependent saturation transfer (CEST). J Magn Reson. 2000; 143:79–87. [PubMed: 10698648]
29. Sherry AD, Woods M. Chemical exchange saturation transfer contrast agents for magnetic resonance imaging. Annu Rev Biomed Eng. 2008; 10:391–411. [PubMed: 18647117]
30. van Zijl PC, Yadav NN. Chemical exchange saturation transfer (CEST): what is in a name and what isn't? Magn Reson Med. 2011; 65:927–948. [PubMed: 21337419]
31. Yoo B, Pagel MD. A PARACEST MRI contrast agent to detect enzyme activity. J Am Chem Soc. 2006; 128:14032–14033. [PubMed: 17061878]
32. Yoo B, Raam MS, Rosenblum RM, Pagel MD. Enzyme-responsive PARACEST MRI contrast agents: a new biomedical imaging approach for studies of the proteasome. Contrast Media Mol Imaging. 2007; 2:189–198. [PubMed: 17712869]
33. Liu G, et al. Monitoring enzyme activity using a diamagnetic chemical exchange saturation transfer magnetic resonance imaging contrast agent. J Am Chem Soc. 2011; 133:16326–16329. [PubMed: 21919523]
34. Liu G, Gilad AA. MRI of CEST-based reporter gene. Methods Mol Biol. 2011; 771:733–746. [PubMed: 21874505]
35. Bar-Shir A, et al. Transforming thymidine into a magnetic resonance imaging probe for monitoring gene expression. J Am Chem Soc. 2013; 135:1617–1624. [PubMed: 23289583]
36. Najjar AM, et al. Molecular-genetic PET imaging using an HSV1-*tk* mutant reporter gene with enhanced specificity to acycloguanosine nucleoside analogs. J Nucl Med. 2009; 50:409–416. [PubMed: 19223410]
37. Greenberg MM. Investigating nucleic acid damage processes via independent generation of reactive intermediates. Chem Res Toxicol. 1998; 11:1235–1248. [PubMed: 9815182]
38. Teoule R, Fouque B, Cadet J. Synthesis and spectroscopic properties of two classes of 5,6-dihydrothymidine derivatives. Action on the Ehrlich's ascites cells thymidine kinase. Nucleic Acids Res. 1975; 2:487–499. [PubMed: 1169761]
39. Judenhofer MS, et al. Simultaneous PET-MRI: a new approach for functional and morphological imaging. Nat Med. 2008; 14:459–465. [PubMed: 18376410]

40. Greenberg MM, et al. DNA damage induced via 5,6-dihydrothymid-5-yl in single-stranded oligonucleotides. J Am Chem Soc. 1997; 119:1828–1839.

41. Barvian MR, Greenberg MM. Independent generation of 5,6-dihydrothymid-5-yl and investigation of its ability to effect nucleic-acid strand scission via hydrogen-atom abstraction. J Org Chem. 1995; 60:1916–1917.

42. Greenberg MM, Matray TJ. Inhibition of Klenow fragment (exo–) catalyzed DNA polymerization by (5R)-5,6-dihydro-5-hydroxythymidine and structural analogue 5,6-dihydro-5-methylthymidine. Biochemistry. 1997; 36:14071–14079. [PubMed: 9369479]

43. Kim M, Gillen J, Landman BA, Zhou J, van Zijl PC. Water saturation shift referencing (WASSR) for chemical exchange saturation transfer (CEST) experiments. Magn Reson Med. 2009; 61:1441–1450. [PubMed: 19358232]

44. Lipton MF, Sorensen CM, Sadler AC, Shapiro RH. Convenient method for the accurate estimation of concentrations of alkyllithium reagents. J Organomet Chem. 1980; 186:155–158.

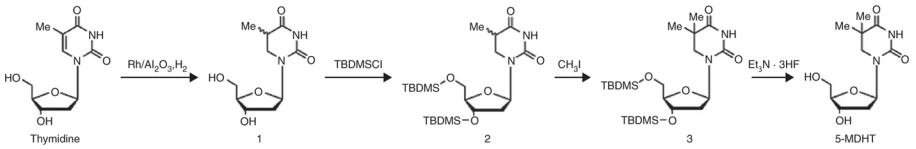

Figure 1.

Synthetic scheme for 5-MDHT. The entire synthesis of 5-MDHT from thymidine as the starting material. $Et_3N{\cdot}3HF$, triethylamine trihydrofluoride; Me, methyl.

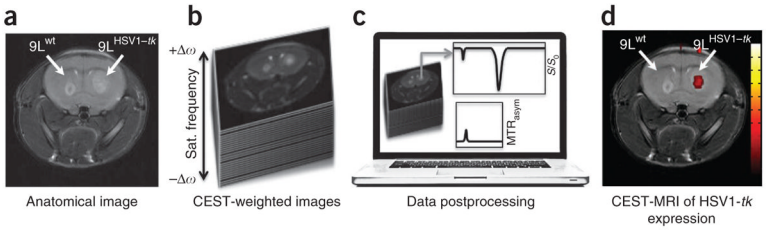

Figure 2.

CEST-MRI data acquisition and processing. (**a**) T_2-weighted image of a representative coronal slice of a mouse brain transplanted with $9L^{wt}$ and $9L^{HSV1\text{-}tk}$ cells, showing the ROI for CEST-MRI. (**b**) A series of CEST-weighted images acquired from +Δ to −Δfrequency offsets from the water resonance. (**c**) Voxel-by-voxel image analysis of the CEST data obtained at **b**. (**d**) CEST map (or MTR_{asym} map) obtained after processing the data from **c** overlaid on the anatomical image in **a**. Adapted with permission from ref. 35. $9L^{wt}$, wild-type 9L rat glioma cells; $9L^{HSV1\text{-}tk}$, HSV1-*tk*–expressing 9L cells.

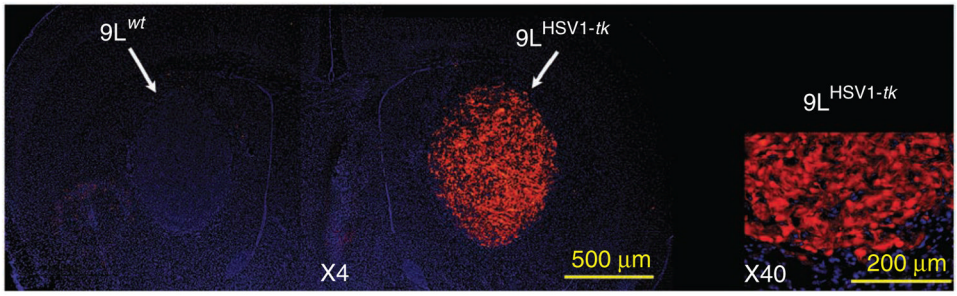

Figure 3.
Histological validation of HSV1-*tk* expression. Immunostaining of a perfused mouse brain coronal section. Staining for HSV1-*tk* (anti-V5 antibody in red) overlaid on DAPI staining (blue) at low (×4) and high (×40) magnifications. Adapted with permission from ref. 35.

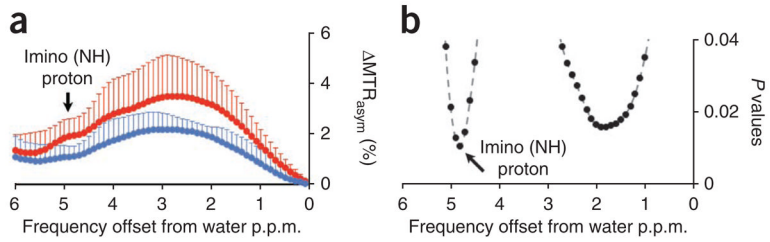

Figure 4.

In vivo detection of the imino proton in $9L^{HSV1\text{-}tk}$. (**a**) ΔMTR_{asym} plots of $9L^{wt}$ (blue) and $9L^{HSV1\text{-}tk}$ (red) (mean ± s.d.; $n = 8$ mice). Arrow points to the local maximal $\Delta\ MTR_{asym}$ and represents the imino proton at 5 p.p.m. after accumulation of **2** in a $9L^{HSV1\text{-}tk}$ tumor. MTR_{asym} ($MTR_{asym} = 100 \times [S^{-\Delta\omega} - S^{\Delta\omega}]/S_0$) was calculated from a complete CEST spectrum (from −6 p.p.m. to +6 p.p.m.; S_0 image without saturation). (**b**) *P* values for each $\Delta\omega$ (Student's *t* test, unpaired, two-tailed) comparing the ΔMTR_{asym} of $9L^{wt}$ or $9L^{HSV1\text{-}tk}$ tumors in the examined mouse brains. The lowest *P* value was obtained at 5 p.p.m. frequency offset from water (black arrow). Adapted with permission from ref. 35.

TABLE 1

Troubleshooting table.

Step	Problem	Possible reason	Possible solution
1–10	Poor conversion of thymidine to 5,6-dihydrothymidine (**1**)	Low efficiency of the catalyst used	Add more catalyst Use new catalyst
		Low H_2 pressure	Prevent H_2 from leaking along the reaction and check the H_2 pressure with an appropriate gauge
		Reaction time was too short	Monitor conversion by TLC (Step 6) and maintain reaction until completion, as reaction time may vary. The reaction mixture may be stirred overnight (up to 18 h) if completion is not achieved in a shorter time
17–25	Unsatisfactory yield of 3′,5′-*O*-bis (*tert*-butyldimethylsilyloxy) 5,6-dihydrothymidine (**2**)	Decomposition of TBDMSCl	Use dry conditions for the reaction and keep it under argon at all times
		Mono (*tert*-butyldimethylsilyloxy) 5,6-dihydrothymidine as main product	Use a higher molar ratio of TBDMSCl to compound **1**, i.e., 3–4 equivalents Add more imidazole
26–33	Unsatisfactory yield of 3′,5′-*O*-bis(*tert*-butyldimethylsilyloxy)-5-methyl-5,6-dihydrothymidine (**3**)	Low concentration of active *sec*-BuLi in the cyclohexane solution	Titrate *sec*-BuLi using 1,3-diphenylacetone *p*-tosylhydrazone to determine *sec*-BuLi molarity[44]. Use corrected volume to achieve 2.5 equivalents
		Methylation on other positions	Perform a low-scale reaction to adjust conditions Keep the reaction temperature at −78 °C at all times Do not exceed 1 h of stirring after *sec*-BuLi addition
		Compound **2** and THF are not dry	Make sure that your reagents are dry before using them in the reaction
34, 35	Unsatisfactory purity of 3′,5′-*O*-bis(*tert*-butyldimethylsilyloxy)- 5-methyl-5,6-dihydrothymidine (**3**)	Poor separation between reagent and product using silica gel column	Use a higher weight ratio of crude product to silica gel (>1:100) Perform a second separation procedure to increase purity
36–38	Uncompleted deprotection of compound **3**	Low quality of triethylamine trihydrofluoride	Monitor conversion by TLC (Step 37) and maintain the reaction until completion Use more triethylamine trihydrofluoride
39, 40	Triethylamine impurities in the product (5-MDHT)	Triethylamine is eluting from the silica gel column with 5-MDHT	Perform another purification step with a higher weight ratio of crude product to silica gel (>1:100)
45	Shimming cannot be adjusted	Animal position	Re-position the animal so that the ROI is set as close to the magnetic field isocenter as possible
48	CEST contrast is not uniform across the same sample or the same biological compartment	B_1 inhomogeneity	Re-position the animal as close as possible to the center of the transmitter RF coil to minimize B_1 inhomogeneity